Selective Self Assembly of Glutamate Molecules on Polyelectrolyte Multilayers

ARTICLE *in* THE JOURNAL OF PHYSICAL CHEMISTRY B · MARCH 2012

Impact Factor: 3.3 · DOI: 10.1021/jp2104648 · Source: PubMed

5 AUTHORS, INCLUDING:

Neelima Paul
Technische Universität München
29 PUBLICATIONS **228** CITATIONS
SEE PROFILE

Amitesh Paul
Technische Universität München
82 PUBLICATIONS **562** CITATIONS
SEE PROFILE

Martin Kreuzer
Catalan Institute of Nanoscience and Nanotec…
16 PUBLICATIONS **48** CITATIONS
SEE PROFILE

Martha Ch. Lux-Steiner
Helmholtz-Zentrum Berlin
593 PUBLICATIONS **8,003** CITATIONS
SEE PROFILE

THE JOURNAL OF PHYSICAL CHEMISTRY B

Article

pubs.acs.org/JPCB

Selective Self Assembly of Glutamate Molecules on Polyelectrolyte Multilayers

N. Paul,*[,†] A. Paul,[‡] R. Steitz,[†] M. Kreuzer,[†] and M. Ch. Lux-Steiner[†]

[†]Helmholtz-Zentrum Berlin, Hahn-Meitner-Platz 1, 14109 Berlin, Germany

[‡]Technical University Munich, Physics-Department, Lehrstuhl for Neutronenstreuung, James-Franck-Strasse. 1, 85748 Garching, Germany

ABSTRACT: The adsorption behavior of neurotransmitter biomolecule, glutamate, on terminal poly-(allylamine)hydrochloride (PAH) polyelectrolyte multilayer is compared with its adsorption on a terminal poly(styrenesulfonate) (PSS) polyelectrolyte multilayer. Using X-ray and neutron reflectivity experiments, the internal structure of such a supramolecular film has been revealed with high resolution and the volume fraction of the adsorbed glutamate is determined. It has been shown that the glutamate binds only to the terminal PAH multilayer. Multiple attenuated total reflection infrared spectroscopy indicates that glutamate is electrostatically physisorbed on PAH surface in the zwitterionic form. Index matching neutron experiments have been done where the scattering length density of the solvent is varied, by changing the ratio of heavy water and light water, until it completely matches with that of the polyelectrolyte layer. The resulting absorption of the glutamic acid leads to changes in scattering profile which are analyzed and it is seen that the adsorption is restricted only to the surface layers. On the other hand, terminal poly(styrenesulfonate) multilayers show resistance toward glutamate. Such repulsion and adsorption between the neurotransmitter and polyelectrolytes could be potentially used in a variety of medicinal applications.

INTRODUCTION

The self-assembly of organic molecules on metal/oxide layers, with a well-defined supramolecular structure, has progressed rapidly in recent years and found applications at the forefront of science and technology like biomaterials,[1] hybrid organic–inorganic nano-objects,[2] or nanoelectronics.[3] Toward a similar goal, the layer-by-layer (LBL) assembly method[4] for the design of polyelectrolyte multilayers (PEMs) has attracted extensive attention as a highly useful way in assembling a number of organic and inorganic architecture assemblies. As their adsorption properties extend to proteins,[5] DNA[6] and nanoparticles,[7] many possibilities open up to design neural implant surfaces aimed at inducing different biological responses from neural tissues and the extracellular fluids. Such specially designed polyelectrolyte layers would be exposed to aminoacids like glutamate (GA) which is ubiquitous in tissue extracellular fluids due to its use as a building block of proteins. This requires detailed understanding of interactions of aminoacids and PEMs. However, direct interactions between neurotransmitter molecules (e.g., glutamate) and polyelectrolyte multilayers are sufficiently unexplored.

Reflectivity techniques have proved to be the most promising techniques for studying the internal structure of PEM films.[8,9] In this paper, we present results of X-ray reflectivity (XRR), neutron reflectivity (NR), and that of a complementary technique of attenuated total reflection (ATR) Fourier Transform infrared (FTIR) spectroscopy. Our measurements explore direct interactions of glutamate (in aqueous solutions) with two different surfaces: a polycationic $Si/SiO_2/PEI/(PSS/PAH)_8$ layer and a polyanionic $Si/SiO_2/PEI/(PSS/PAH)_8PSS$ layer and give insight into the internal layer structure with chemical identification.

At room temperature and pH 7, glutamic acid exists in the zwitterionic form which is written as $COO^-.CH_2.CH_2.NH_3^+.CH.COO^-$, known as glutamate. The chemical structures of glutamate and poly(allylamine)-hydrochloride and poly(styrenesulfonate) are shown in Figure 1. Glutamic acid has two known polymorphs. The unit cell of the alpha polymorph is close to cubic ($7.1 \times 8.3 \times 10.3$ Å^3) while the unit cell of the beta polymorph has a more elongated shape ($5.2 \times 6.9 \times 17.3$ Å^3).[10,11] There have been a few studies on adsorption of glutamic acid from a gaseous state onto solid metal surfaces. On adsorption, systems of that type, display

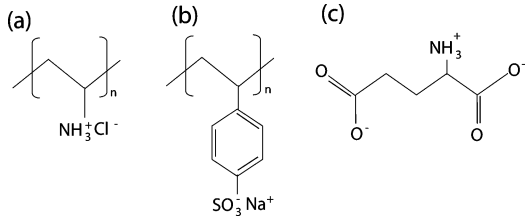

Figure 1. Structures of the chemicals used at pH 7 (a) poly-(allylamine)hydrochloride (PAH), (b) poly(styrenesulfonate) (PSS), and (c) glutamate.

Received: October 31, 2011
Revised: January 25, 2012
Published: March 16, 2012

ordered adlayer structures with the chemisorbed molecules in either the anionic form ($H_2N{\cdot}CR{\cdot}COO^-$, where R represents some functional group) or in the zwitterionic form. For example, (S)-glutamic acid is found to bind to Ag(110) mainly in the anionic form.[12] In contrast, Stewart and Fredericks[13] conclude that glutamic acid (and the other amino acids) adsorbs to roughened silver surfaces in the zwitterionic form. There are a large number of prospective applications in medicine for such study of the neurotransmitter where it can be resisting off or attracting to the liquid/solid interface depending on the charge of the solid surface. For some materials, biological incompatibility occurs because of unwanted neurotransmitter adsorption while in others the spontaneous adsorption of the neurotransmitter is preferable to restore the function of damaged neuronal cells.[14] A study of the neurotransmitter, glutamate, in its negatively charged state is necessary also to understand the critical and complex interactions of peptides and proteins with surfaces.[15]

METHODS

The X-ray reflectivity experiments were performed on a triple axis diffractometer using Cu Kα (λ = 1.54 Å) radiation. The resolution of the instrument was set to δq_z = 0.003 Å^{-1}. Details on this instrument and its operational mode can be found elsewhere.[16] The neutron reflectivity experiments were performed on the reflectometer V6 at the Helmholtz Zentrum Berlin. In both cases the reflectivity, R, was recorded as a function of scattering vector, $q_z = (4\pi/\lambda) \sin\theta$, and θ is the reflection angle. V6 is a monochromator-based instrument. A neutron wavelength of λ = 4.66 Å was selected by a pyrolytic graphite crystal PG 002 located in the incident white beam. The angular resolution was set by a slit system on the incident side resulting in scattering vector resolution, δq_z, of 0.001 Å^{-1} for q_z < 0.0518 Å^{-1}, and 0.002 Å^{-1} otherwise. The scattered neutrons were recorded stepwise with a ^{3}He-detector. Background intensity was measured simultaneously with a second ^{3}He-detector, offset from the one at specular position by $\delta(2\theta)$ = 0.44°. The measured intensity was corrected for varying footprint of the incident beam on the interface as a function of incident angle θ. Further details on V6 can be found elsewhere.[17,18] A home-built flow cell especially designed for neutron reflectivity experiments at the solid−liquid interface was used.[19]

The interference of X-rays (or neutrons) scattered at the Si/PEM and the PEM/air (or PEM/D_2O) interfaces gives rise to a series of oscillations with pronounced maxima and minima in R (Kiessig oscillations). The spacing between neighboring Kiessig fringes corresponds to the PEM layer thickness, the amplitude of the oscillations couples to the gradient in the scattering length density (SLD) and the damping of the oscillations to the interfacial roughness. Note that the internal structure of PEM is amorphous, as shown in seminal work by Schmitt et al[8] and Lösche et al.[9] Both X-ray reflectivity and neutron reflectivity data were fitted by applying the optical matrix method, resulting in a layer thickness, an interface roughness and a scattering length density (NR) or electron density (XRR), which are the fitting parameters. The measured background was added to model reflectivity curves as a fixed parameter. The model reflectivity profile is calculated and compared to the measured one, then the model is adjusted by a change in the fitting parameters to best fit the data.

For Fourier Transform infrared spectroscopy, a commercial FTIR device 113v (Bruker GmbH, Germany) equipped with an ATR unit was used. The ATR geometry allows for multiple reflections, which provide an enhanced sensitivity to chemical identification of molecular species at the solid/liquid interface. It provides an infrared sensitivity of the order of 10% of an adsorbate monolayer and the possibility of monitoring species that absorb in the water absorption range.[20]

SAMPLE PREPARATION

The chemicals PSS (M_w = 70 000 g mol^{-1}), poly(ethyleneimine) PEI (M_w = 750 000 g mol^{-1}), PAH (M_w = 70 000 g mol^{-1}), and glutamic acid were purchased from Sigma-Aldrich while deuterated poly(styrene sodium sulfonate), dPSS (M_w = 80 800 g mol^{-1}) was purchased from Polymer Standards Service (Mainz, Germany). Polymer solutions using 1 M NaCl were prepared in Milli-Q water or D_2O. Polyelectrolyte films were deposited on Si substrates using LbL protocol. The substrate was dipped in a solution of PEI (which was the initial layer) for 20 min. This was followed by alternate immersions (20 min) in solutions of PSS and PAH. Each immersion was followed by a washing step of 2 min soaking per beaker in three consecutive beakers of Milli-Q water. This adsorption/washing cycle was repeated for each adsorption step until the desired number of layers had been reached. For neutron reflectivity, PSS was replaced by dPSS to increase the scattering contrast. The Si wafers used for NR were ordered from Siliciumbearbeitung Andrea Holm (Tann, Germany). They have a size of 8 cm ×5 cm ×1.5 cm, with one of the two large surfaces being polished. The optically polished Si ATR crystal (2 × 45°, 50−0.2 mm ×10−0.1 mm ×3 mm) for IR spectroscopy was ordered from Korth Kristalle. Polyelectrolytes were deposited to this crystal by inserting polymer solutions in the ATR liquid cell using similar LbL protocol. Prior to depositions, all wafers were cleaned by heating them in a 1:1:5 mixture of H_2O_2 (30%), NH_3 (30%), and H_2O followed by intensive rinsing with pure water (modified RCA cleaning procedure).[21]

RESULTS AND DISCUSSION

FTIR Spectroscopy. Utilizing Fourier Transform infrared spectroscopy, the presence of an aminoacid on a sample can be confirmed by detecting the vibration modes of the specific functional groups in its chemical structure. Moreover, in molecules like glutamate, the carboxylate and primary amine groups change their protonation state with pH. Thus, the spectroscopic studies are useful also for determining the chemical structure on adsorption. Lanzilotta et al.[22] had studied the glutamic acid in H_2O using infrared spectroscopy and could identify most of the functional groups as a function of pH. At pH 6, they had recognized the glutamate by the characteristic stretching vibrations at 1400 cm^{-1}, 1556 cm^{-1} and 1593 cm^{-1}.

In Figure 2, we show the FTIR spectra for 1 M glutamate in H_2O and 1 M glutamate in D_2O. One can see a peak at 1400 cm^{-1}, due to the symmetric vibrations of the two COO^- groups. The peaks at 1560 cm^{-1} and 1610 cm^{-1} are due to asymmetric stretching vibrations of the COO^- and due to the bending vibrations of NH_3^{+1} respectively. For both solvents, the GA at pH 7 does not show any peak at 1720 cm^{-1} which would correspond to the position of the COOH functional group. In our investigations with PEMs, water (H_2O) was replaced by heavy water (D_2O) for better quality of the spectra. In this way, the peak due to the bending vibrations of water at 1630 cm^{-1} gets shifted to lower wavenumbers and the bending vibrations

dx.doi.org/10.1021/jp2104648 | J. Phys. Chem. B 2012, 116, 4492−4499

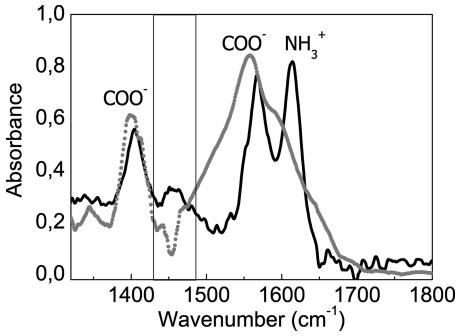

Figure 2. ATR-FTIR spectrum of 1 M of glutamate in H_2O (gray dotted line) and 1 M of glutamate in D_2O solvent (black line) with H_2O or D_2O solvent as reference spectrum. The shoulder peak around 1600 cm^{-1} in spectrum of glutamate in H_2O can clearly be resolved by replacing H_2O by D_2O. The rectangle corresponds to region of the adsorption edge of the Si which causes noise in spectrum.

of the amine groups and the stretching vibrations of the carboxylate groups can be clearly seen. The shifting to lower frequencies is because the mass of attached deuterium atoms in heavy water is heavier than the mass of the attached hydrogen atoms in water and thus the bonds absorb at lower IR frequencies.

The ATR−FTIR spectroscopy difference spectrum between a $Si/SiO_2/PEI/(PSS/PAH)_8$ surface (black line) before and after immersion in a 1 M solution of glutamate, both against a D_2O solvent, is shown in Figure 3. The absorption peaks at

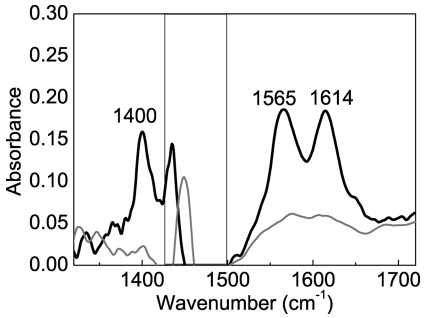

Figure 3. ATR-FTIR spectrum of $Si/SiO_2/PEI/(PSS/PAH)_8/GA$ (black line) against the reference $Si/SiO_2/PEI/(PSS/PAH)_8$, in D_2O solvent strongly indicates the presence of immobilized glutamate whereas the spectrum of $Si/SiO_2/PEI/(PSS/PAH)_7/PSS/GA$ (gray line) against the reference $Si/SiO_2/PEI/(PSS/PAH)_7/PSS$ cannot verify the presence of glutamate. The rectangle corresponds to region of the adsorption edge of the Si which causes noise in spectrum.

1614 cm^{-1}, 1565 cm^{-1} and 1400 cm^{-1} not only identify glutamate at the $Si/SiO_2/PEI/(PSS/PAH)_8$ surface but also indicate that glutamate is adsorbed in a state which preserves the carboxylate symmetric stretching mode at 1400 cm^{-1} and the asymmetric carboxylate stretching mode at 1565 cm^{-1} respectively. Moreover, the wavenumber splitting of the stretches of the carboxylate groups is not significantly changed upon adsorption. This implies most likely an electrostatic nature of the binding between the carboxylate groups of the glutamate and the positively charged terminal PAH layer. The band at 1593 cm^{-1} was attributed by Lanzilotta et al. as partially due to NH_3^+ and was not seen by them at higher pH due to its reduction to NH_2. That we also observe a peak at 1614 cm^{-1} suggests that the adsorbed glutamate has NH_3^+ and thus the dominant adsorbed species is most likely zwitterionic glutamate. On the other hand, the difference spectrum between a $Si/SiO_2/PEI/(PSS/PAH)_7/PSS$ surface (gray line) before and after immersion in a 1 M solution of glutamate, also shown in Figure 3 cannot verify the presence of glutamate.

X-ray Reflectivity. The preparation of the substrates for the X-ray reflectivity was done in the following way; on the substrate (A) (or (B)), initially a precursor layer of the polyelectrolyte $Si/SiO_2/PEI/(PSS/PAH)_7PSS$ (or $Si/SiO_2/PEI/(PSS/PAH)_8$) was grown on the entire Si wafer. Then, only the right half was dipped in the 1 M glutamate solution for 1 h, rinsed extensively with water and dried. Thus the Si substrates were prepared in such a way that the left halves of the Si wafers had the precursor PEM and the right halves had the precursor PEM plus GA. Both substrates were kept under similar dry conditions and X-ray reflectivity measurements were performed consecutively on both halves of each of the two substrates.

Figure 4a shows the X-ray reflectivity curves from the two halves of the substrate (A); $Si/SiO_2/PEI/(PSS/PAH)_7PSS$ and

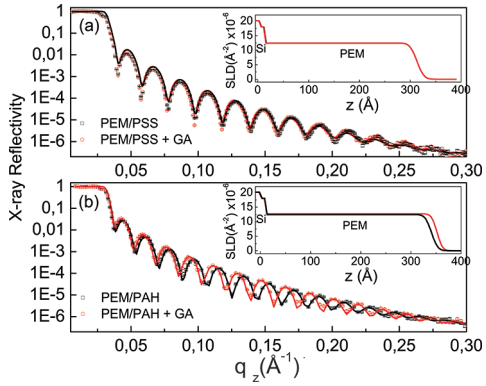

Figure 4. X-ray reflectivity data of (a) $Si/SiO_2/PEI/(PSS/PAH)_7/PSS$ and (b) $Si/SiO_2/PEI/(PSS/PAH)_8$ against air before (black open circles) and after (red open circles) immersion in glutamate solution and their fits (lines). The fits correspond to the absorption of a 12 ± 3 Å thick GA layer on $Si/SiO_2/PEI/(PSS/PAH)_8$. The insets are the corresponding scattering length density profiles. The interfacial roughnesses at the PEM−air interface were 12 Å.

$Si/SiO_2/PEI/(PSS/PAH)_7PSS$ exposed to the glutamate solution. Data from both halves overlap for almost the entire q_z range measured. The results of the fitting of the X-ray reflectivity data are given in Table 1. The interfacial roughness at the PEM/air interface was about 12 Å . From the fits, we find a thickness increase of 1 ± 3 Å . Quantitatively, the value is in the range of the resolution of the measurement. So it is difficult to attribute this thickness increase to a glutamate layer unambiguously. Moreover, it is too small to accommodate

Table 1. Thicknesses and Scattering Length Densities of the Specimens as Obtained from the Least Square Fits to the X-ray Reflectivity Data Both before (Denoted as d and ρ) and after Addition of Glutamate (Denoted as d' and ρ')

XRR	d (Å) ± (3)	ρ (× 10^{-6} Å^{-2}) ± (0.1)	d' (Å) ± (3)	ρ' (× 10^{-6} Å^{-2}) ± (0.1)
		$Si/SiO_2/PEI/(PSS/PAH)_8$		
PEM	331	12.4	343	12.7
		$Si/SiO_2/PEI/(PSS/PAH)_7PSS$		
PEM	296	12.5	297	12.5

dx.doi.org/10.1021/jp2104648 | J. Phys. Chem. B 2012, 116, 4492−4499

the minimum configuration of glutamate. In contrast, the X-ray reflectivity curves from the $Si/SiO_2/PEI/(PSS/PAH)_8$ and the $Si/SiO_2/PEI/(PSS/PAH)_8$ exposed to glutamate solution (Figure 4b) shows a distinct shift of the Kiessig fringes to lower q_z due to the adsorbed GA layer. The fits to the data correspond to an increase in thickness of 12 ± 3 Å, which is close to the expected footprint of a (S)-GA molecule.[12] This indicates that atleast a layer of glutamate is deposited on the $Si/SiO_2/PEI/(PSS/PAH)_8$ surface.

Neutron Reflectivity. While the X-ray reflectivity were carried out against air in the "dry" state, the neutron reflectivity experiments were performed in the "wet" state. Neutron reflectivity was done in addition to X-ray reflectivity with the aim of estimating the thickness of adsorbed glutamate layer in the swollen state of the PEMs. Two different approaches were made to get a convincing evidence of glutamate adhesion on PEM.

Contrast Enhanced Method. To cancel any possibility of error in glutamate thickness estimation by an unequal expansion of the PEM along the length of the Si substrate, we followed a slightly different measurement in neutron reflectivity. On the Si substrates, which were used for neutron reflectivity, the PEM precursor was deposited on the entire Si block and the initial neutron reflectivity measurement against pure solvent was conducted. In the next step, the substrate was exposed to glutamate solution in situ for 1 h, after which a glutamate free solvent was introduced and then the final neutron reflectivity measurement was taken. In this way, the reflectivity measurements are performed over the same area before and after glutamate exposure. This was particularly possible because of the usage of a liquid cell setup for neutron reflectivity.

The scattering contrast of the PEM for neutrons is dependent on the mole-fraction of deuterium in the solvent due to large amount of solvent absorption by the PEM layer.[23] To achieve a good neutron scattering length density (SLD) contrast, the ratio of D_2O:H_2O in the solvent was varied in a series of neutron reflectivity experiments. The resulting spectra are shown in Figure 5. For clarity, the data for 1:1 H_2O:D_2O (HDO) and H_2O have been shifted down by a factor of 2 and 20 respectively. It can be seen that the Kiessig oscillations have the lowest amplitude with the H_2O solvent and the maximum amplitude (and the best contrast) with the HDO solvent. Therefore we chose HDO solvent for further experiments.

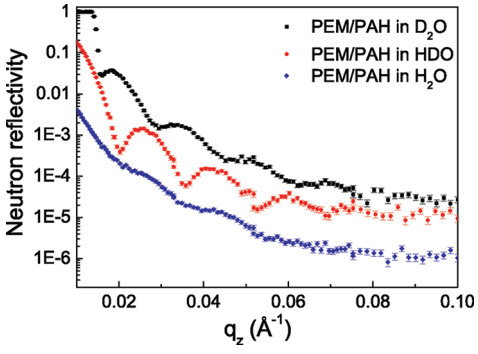

Figure 5. Neutron reflectivity data of $Si/SiO_2/PEI/(dPSS/PAH)_8$ against D_2O (black rectangle), HDO (red circle) and H_2O solvent (blue diamond). The HDO solvent gives the best neutron scattering contrast. The data with HDO and H_2O solvent have been shifted down by a factor of 2 and 20 for clarity.

In Figure 6, we show the NR data of $Si/SiO_2/PEI/(dPSS/PAH)_8$ and $Si/SiO_2/PEI/(dPSS/PAH)_8dPSS$ against HDO

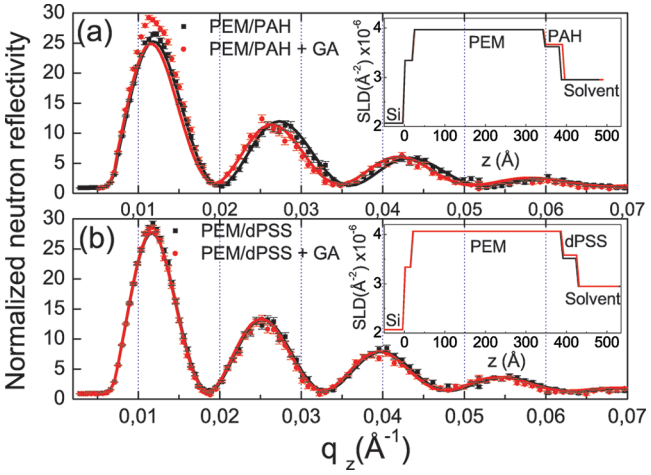

Figure 6. Neutron reflectivity (The data are normalized on the Fresnel reflectivity of the ideal silicon/liquid interface) of (a) $Si/SiO_2/PEI/(dPSS/PAH)_8$ and (b)$Si/SiO_2/PEI/(dPSS/PAH)_8/dPSS$ against HDO solvent before (black circles) and after (red circles) immersion in glutamate solution and their fits (red/black line for red/black circles). The insets are the corresponding scattering length density profiles.

solvent before and after exposure to glutamate solution. The data are normalized on the Fresnel reflectivity of the ideal silicon/liquid interface. With every D_2O/H_2O mixture (1:1 or 1:0 D_2O:H_2O), the Kiessig oscillations observed for $Si/SiO_2/PEI/(dPSS/PAH)_8$ shift to lower q_z upon incubation of the substrate with a 1 M solution of glutamate, indicating an increase in layer thickness due to glutamate adsorption. In contrast, the Kiessig oscillations observed for $Si/SiO_2/PEI/(dPSS/PAH)_8dPSS$ remain unchanged after incubation of the substrate with glutamate solution, indicating no glutamate adsorption.

The neutron reflectivity data are analyzed following the two models as sketched in Figure 7. In model A, it is assumed that the glutamate could diffuse into the entire PEM bulk and replace a part of the solvent. The PEM and glutamate layer were modeled as one layer, varying the initial thickness as well as the previously obtained scattering length density value for the PEM in the fitting. According to model B, the glutamate (GA) layer is expected to attach only to the surface of the PEM and therefore an additional separate surface layer (PE+GA) was included. Here, the thickness and SLD values of the bulk PEM were fixed while the SLD and thickness of the surface layer (PE +GA) layer was allowed to vary after exposure to glutamate solution.

The PEM is fitted as a single box for Model A, as in most of the literature[5,9,25,24] which state that (due to the strong chain interdigitation) it is impossible to resolve single, neighboring polyelectrolyte layers in neutron reflectivity. The results of the fitting are shown in Table 2. However, to describe the model B, we have introduced for the PEM, a surface PE layer, in addition to the single PEM block. This surface PE layer is in a different environment as compared to the PE layers in the bulk of the PEM. The surface PE layer is still interdigitated with the bulk PEM on one (inner) side but has now only the solvent on the other (outer) side with loops and tails extending into the adjacent liquid phase. Hence, the composition, i.e. the volume

dx.doi.org/10.1021/jp2104648 | J. Phys. Chem. B 2012, 116, 4492–4499

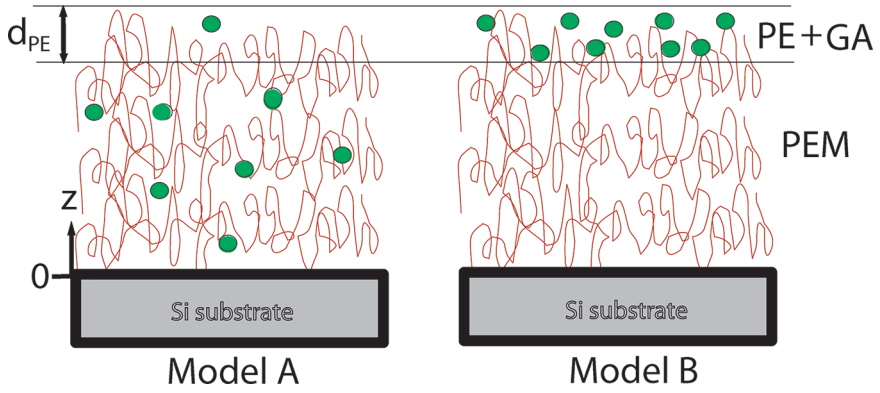

Figure 7. Schematic of Model A (diffusion) and Model B (separate surface layer) where green circles represent possible positioning of glutamate molecules on the PEM (red) after adsorption. These model diagrams picturise the depth dependence of glutamate in PEM.

Table 2. Thicknesses and Scattering Length Densities of the Specimens As Obtained from the Least Square Fits of Model A to the Neutron Reflectivity Data Both before (Denoted as d and ρ) and after Addition of GA (Denoted as d' and ρ')

NR	d (Å) ± (3)	ρ (× 10^{-6} Å^{-2}) ± (0.1)	d' (Å) ± (3)	ρ' (× 10^{-6} Å^{-2}) ± (0.1)
		$Si/SiO_2/PEI/(dPSS/PAH)_8$		
PEM	345	3.9	354	3.9
solvent		2.9		2.9
		$Si/SiO_2/PEI/(dPSS/PAH)_8/dPSS$		
PEM	385	4.1	386	4.1
solvent		2.9		2.9

Table 3. Thicknesses and Scattering Length Densities of the Specimens As Obtained from the Least Square Fits of Model B to the Neutron Reflectivity Data Both before (Denoted as d and ρ) and after Addition of GA (Denoted as d' and ρ')

NR	d (Å) ± (3)	ρ (× 10^{-6} Å^{-2}) ± (0.1)	d' (Å) ± (3)	ρ' (× 10^{-6} Å^{-2}) ± (0.1)
		$Si/SiO_2/PEI/(dPSS/PAH)_8$		
PEM	320	4.0	320	4.0
PE surface layer	39	3.6	47	3.7
solvent		2.9		2.9
		$Si/SiO_2/PEI/(dPSS/PAH)_8/dPSS$		
PEM	371	4.0	371	4.0
PE surface layer	36	3.5	37	3.5
solvent		2.9		2.9

fractions of PE and solvent in the surface region might differ from the equilibrium situation in the bulk of the PEM. In consequence and for different SLD of PE and solvent, the SLD of the film surface layer (now labeled PE) may differ from that of the film bulk (PEM). Recent literature has also reported that the thickness of such surface PE layer could differ from the corresponding bulk value.[25] Details on our fitting strategy can be found here.[26]

From the data analysis, following Model A and B, we obtained a thickness of the adsorbed layer of 9 ± 3 Å and 8 ± 3 Å, respectively, for $Si/SiO_2/PEI/(dPSS/PAH)_8$. Note this is in a similar range to the value of the adsorbed layer from the XRR results. The two values do not exactly match due to the fact that they are measured in the wet and dry state respectively. However they are in good agreement taking into account the error bars and the different humidity conditions. We give the fitted parameters according to Model A and B in Tables 2 and 3. Fits based on Model B offer less errors (lower chi^2) as compared to those based on Model A. For $Si/SiO_2/PEI/(dPSS/PAH)_8$ in a HDO solvent, the SLD of the surface PEM layer was 3.6 × 10^{-6} Å^{-2} and increased to 3.7 × 10^{-6} Å^{-2} on addition of the GA which has a SLD of 3.2 × 10^{-6} Å^{-2}. This slight increase was due to the higher SLD of GA as compared to the solvent (2.9 × 10^{-6} Å^{-2}), which it partially replaced in the surface layer of the PEM.

On the contrary, the neutron reflectivity curves of the $Si/SiO_2/PEI/(dPSS/PAH)_8/dPSS$ surface before and after incubation in glutamate solution, do not show any shift in the Kiessig oscillations as shown in Figure 6(b). The best fits for PSS-terminated PEM layers calculate a thickness increase of 1 ± 3 Å (Model A and B). This value is obviously within the error bars and also too small to accommodate the minimum configuration of GA (at least 5 Å). Therefore we can conclude that there was no adsorption of glutamate on the wet negatively charged $Si/SiO_2/PEI/(dPSS/PAH)_8/dPSS$ surface.

Generally, there is spontaneous adsorption of organic molecules such as proteins and aminoacids from aqueous solutions onto solid surfaces.[27−29] The driving forces for such interaction are hydrophobic, electrostatic, entropic and van der Waals interactions, depending on the protein structure and the nature of the solid surface.[30−33] Consequently, adsorption is also observed when both organic molecules and the surface have the same charge, i.e. under electrostatic repulsion. For example, although bovine serum albumin (BSA) and silica are both negatively charged, BSA adsorbs to silica from aqueous solutions.[34−36,38] On the other hand, positively charged lyzozyme also adsorbs to silica.[30,31] On surfaces such as PAH/PSS multilayer, both BSA and the lysozyme adsorb from solutions.[38] Earlier studies in which the zeta-potentials were determined, revealed that the multilayers terminating with a PSS (PAH) layer exhibit a negative (positive) zeta-potential.[37] It is thus expected that glutamate, being a polar aminoacid having two deprotonated carboxylate groups and a protonated amino group at pH 7, and a net charge of −1, interacts strongly with the positively charged multilayer under attractive electrostatic forces. In case of interaction with the negatively charged polyelectrolyte, the binding is not observed which is due to repulsive electrostatic forces. This implies that in the system studied here, the electrostatic forces dominate over other interactions. Moreover, while electrostatic attraction could involve either single or several layers of the adsorbed species, this study clearly demonstrates binding of atleast a single layer of glutamate. The presence of the polyelectrolytes seems, as previously observed for fibrinogen,[38] to prevent intermolecular

dx.doi.org/10.1021/jp2104648 | J. Phys. Chem. B 2012, 116, 4492−4499

interactions and, thus, glutamate aggregation at ambient temperature. This is in accordance with our explanation that the adsorption of glutamate leads to charge reversal of the interface.

Index Matched Water Method. To confirm if the glutamate diffuses into the $Si/SiO_2/PEI/(dPSS/PAH)_8$ (Model A) or attaches to its surface (Model B), an additional set of neutron reflectivity experiments using index matched water (IMW) were performed. By suitable selection of the amount of D_2O in the solvent, it was possible to match the scattering length density of the solvent to that of the PEM layer and make the Kiessig oscillations disappear.[39]

Note that, due to its enhanced sensitivity to any adsorbed layer, this is a useful technique to detect even a monolayer of adsorbed molecules on PEMs, given their scattering length density differs from that of index matched water. The $Si/SiO_2/PEI/(dPSS/PAH)_8$ (PEM layer) was made invisible by contrast matching so that we were left with a simple Fresnel type interface Si/PEM(invisible) = Si/IMW.

A series of contrast matching experiments were performed to determine the match point of the PEM layer. The $Si/SiO_2/PEI/(dPSS/PAH)_8$ was exposed to solvents containing different ratios of D_2O and H_2O, the corresponding neutron measurement was done and the data were fitted to extract the scattering length density of both the PEM and of the corresponding solvent. The results are shown in Figure 8.

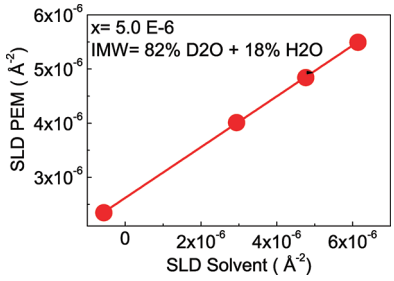

Figure 8. Calculation of the PEM matchpoint (5.0×10^{-6} Å^{-2}) from results of neutron reflectivity fitting to $Si/SiO_2/PEI/(dPSS/PAH)_8$ in solvents having different ratios of D_2O/H_2O.

The scattering length densities of the PEM layer and the solvent subphase were precisely matching for a solvent containing 82 vol % D_2O and 18 vol % H_2O, corresponding to a scattering length density of 5.0×10^{-6} Å^{-2}. Hence, the well-pronounced Kiessig oscillations for $Si/SiO_2/PEI/(dPSS/PAH)_8$ in a pure D_2O solvent and $Si/SiO_2/PEI/(dPSS/PAH)_8$ in a pure H_2O solvent (virtually) disappeared when the solvent was exactly index matched. In this special case, scattering length densities of both the PEM bulk and the PE surface layer matched with the SLD of the solvent within the resolution of the measurement. This is shown in Figure 9a or c (the data with the black circles). The scattering length density profile (black lines) is also shown in the inset. For the fits based on Model B, we assume the thickness of the surface PE layer to be 39 Å, according to data analysis of $Si/SiO_2/PEI/(dPSS/PAH)_8$ in table 3.

Subsequently, the PEM was then exposed to an index matched water solution containing 1 M glutamate for 1 h and finally to the pure index matched water (i.e., without glutamate). The results from the subsequent neutron reflectivity measurements can be seen in Figure 9a or c (as the red squares). The Kiessig oscillations reappeared! To

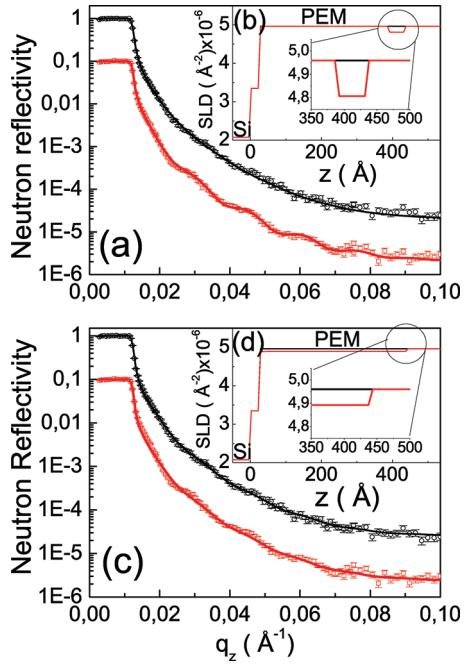

Figure 9. (a) Neutron reflectivity data of $Si/SiO_2/PEI/(dPSS/PAH)_8$ against index matched water solvent before (black circles) and after (red squares) immersion in glutamate solution and their fits (lines)(according to Model B). The Kiessig oscillations reappear after immersion in a glutamate solution. The lower curve has been shifted for clarity. (c) Neutron reflectivity data of $Si/SiO_2/PEI/(dPSS/PAH)_8$ against index matched water solvent before (black circles) and after (red squares) immersion in glutamate solution and their fits (lines)(according to Model A). (b and d) The insets are the corresponding scattering length density profiles (black lines for PEM and red lines for PEM+GA) with magnification in the region of the adsorbed layer.

account for the fact that these oscillations were not due to a slight mismatch of subphase and PEM scattering length density, we checked the position of the total reflection edge and it was the same for both the index matched water solutions, before and after the glutamate adsorption step. In Figure 9a, the data are fitted following Model B. In the inset, the scattering length density of the PE surface layer reduces while its thickness increases. The scattering length density profile (black line) before addition of glutamate could not resolve between the scattering length densities of the bulk PEM and surface PE layer. Although the volume fraction of PE within the surface layer is different from the bulk the scattering length densities of PE and solvent are index matched. Hence there is no contrast for neutrons also for the PE surface layer prior to adsorption of GA. However, once the glutamate is adsorbed, it accommodates itself in the surface PE and changes the scattering length density and the thickness of the surface PE layer. This leads to the appearance of the new box in the scattering length density profile (red line) of Figure 9b. The thickness of the box includes the thickness of the surface PE and the glutamate. In Figure 9c, the data are fitted following Model A. However those fits do not match the data as precisely as the fits based on Model B. In the inset d, after GA adsorption, the scattering length density of the PEM reduces from 5.0×10^{-6} Å^{-2} to 4.9 $\times 10^{-6}$ Å^{-2} and the thickness increases by 12 ± 3 Å . In Table 4, we give the fitted parameters to the neutron reflectivity data obtained by index matching before and after exposure to glutamate according to both Model A and Model B. Though

dx.doi.org/10.1021/jp2104648 | J. Phys. Chem. B 2012, 116, 4492–4499

Table 4. Thicknesses and Scattering Length Densities of the Specimens As Obtained from the Least Square Fits to the Neutron Reflectivity Data Both before (Denoted as d and ρ) and after Addition of Glutamate (Denoted as d' and ρ')

NR	d (Å) ± (3)	ρ ($\times 10^{-6}$ Å^{-2}) ± (0.1)	d' (Å) ± (3)	ρ' ($\times 10^{-6}$ Å^{-2}) ± (0.1)
Si/SiO_2/PEI/(dPSS/PAH)$_8$: Fit with Model A				
PEM	401	5.0	413	4.9
solvent		5.0		5.0
Si/SiO_2/PEI/(dPSS/PAH)$_8$: Fit with Model B				
PEM	361	5.0	361	5.0
surface PE layer	39	5.0	46	4.8
solvent		5.0		5.0

fits from both models indicate an increase in thickness of the PEM, the results also indicate that only box model B can describe the data with reasonable accuracy, as the calculated reflectivity curves for box models A do not superimpose well with the experimental data points (chi^2 is less for Model B). This can be also seen by comparing the fits to the data in Figures 9 (a) and (c). Therefore, we conclude that the glutamate exclusively adsorbs to the surface PE layer and does not diffuse into the PEM bulk. The neutron reflectivity fittings of the observable Kiessig oscillations correspond to a net glutamate thickness of about 7 ± 3 Å .

Further, from the result of the fit based on Model B, it is possible to extract the volume fraction of glutamate which replaces index matched water in the surface PE layer. In the case of index matching, the scattering length density of the PEM is similar to scattering length density of the solvent, which is the reason for the disappearance of the Kiessig fringes of the PEM. Upon adsorption of glutamate, we presume that the only the scattering length density of surface PE layer (and not of the bulk PEM) is changed. Thus it is possible to calculate the volume fraction of the glutamate in the surface layer:

1. $SLD_{surfacePE} = xSLD_{GA} + ySLD_{IMW} + zSLD_{PEM}$ with $x + y + z = 1$
2. $SLD_{PEM} = SLD_{IMW}$, hence $z + y = 1 - x$
3. Therefore, $SLD_{surfacePE} = xSLD_{GA} + (1 - x)SLD_{IMW}$

where x is the volume fraction of glutamate in the surface PE layer. From the fitting of the data in Figure 9a, $SLD_{IMW} = 5.0 \times 10^{-6}$ Å^{-2} and $SLD_{surfacePE} = 4.8 \times 10^{-6}$ Å^{-2}, the theoretically calculated value of glutamate in IMW is 3.7×10^{-6} Å^{-2} which leads to a value of 0.15 as the volume fraction of glutamate in the surface PE. Thus, on adsorption, glutamate replaces 15% of water in the surface PE layer.

CONCLUSION

The interaction of glutamate with polyelectrolyte multilayers has been described in detail, involving two different scattering techniques, X-ray reflectivity and neutron reflectivity, and an absorption spectroscopic technique. In our investigation, we demonstrate that this neurotransmitter deposits exclusively on the terminal poly(allylamine)hydrochloride layer of the polyelectrolyte multilayers against the liquid phase causing an approximate 9 ± 3 Å increase in thickness in the swollen state against excess solvent as well as in the collapsed state after solvent removal. Moreover, the glutamate adsorbs only to the surface of the poly(allylamine)hydrochloride terminated polyelectrolyte multilayer and not to the poly(styrenesulfonate) terminated polyelectrolyte multilayer. In the former case, the carboxylate groups of the glutamate molecules are bound by mainly electrostatic forces to the NH_3^+ groups of the poly(allylamine)hydrochloride surface as concluded from attenuated total reflection infrared spectroscopy. With the contrast matching neutron scattering technique, we have made the polyelectrolyte multilayers virtually invisible and thereby have enhanced the scattering contrast of glutamate adsorbed layer at the surface. By employing the unique combination of neutron reflectivity and infrared spectroscopy we have demonstrated that the internal structure and binding configuration of the adsorbed glutamate at a solid/liquid interface can be studied with high resolution.

AUTHOR INFORMATION

Corresponding Author

*E-mail: neelima.paul@helmholtz-berlin.de. Tel: 0049-89-28912449. Fax:0049-89-28912473.

Notes

The authors declare no competing financial interest.

ACKNOWLEDGMENTS

This work was supported by Bundesministerium für Bildung und Forschung Rahmenprogramm Mikrosystemtechnik.

REFERENCES

(1) Love, J. C.; Estroff, L. A.; Kriebel, J. K.; Nuzzo, R. G.; Whitesides, G. M. *Chem. Rev.* **2005**, *105*, 1103−1170.
(2) Mann, S. *Nat. Mater.* **2009**, *8*, 781−792.
(3) Pennec, Y.; Auwarter, W.; Schiffrin, A.; Weber-Bargioni, A.; Riemann, A.; Barth, J. V. *Nat. Nanotechnol.* **2007**, *2*, 99−103.
(4) Decher, G. *Science* **1997**, *277*, 1232−1237.
(5) Decher, G.; Lehr, B.; Lowack, K.; Lvov, Y.; Schmitt, J. B. *Biosens. Bioelectron.* **1994**, *9*, 677−684.
(6) Lvov, Y.; Decher, G.; Sukhorukov, G. *Macromolecules* **1993**, *26*, 5396−5399.
(7) Fiorito, P. A.; Goncales, V. R.; Ponzio, E. A.; Cordoba de Torresi, S. I. *Chem. Commun.* **2005**, 366−368.
(8) Schmitt, J.; Gruenewald, T.; Decher, G.; Pershan, P. S.; Kjaer, K.; Loesche, M. *Macromolecules* **1993**, *26*, 7058−7063.
(9) Loesche, M.; Schmitt, J.; Decher, G.; Bouwman, W. G.; Kjaer, K. *Macromolecules* **1998**, *31*, 8893−8906.
(10) Lehmann, M. S.; Nunes, A. C. *Acta Crystallogr. B* **1980**, *36*, 1621−1633.
(11) Lehmann, M. S.; Koetzle, T. F.; Hamilton, W. C. *J. Am. Chem. Soc.* **1972**, *94*, 2657−2660.
(12) Jones, T. E.; Baddeley, C. J. *Langmuir* **2005**, *21*, 9468−9475.
(13) Stewart, S.; Fredericks, P. M. *Spectrochim. Acta Part A* **1999**, *55*, 1641−1660.
(14) Zrenner, E.; Lux-Steiner, M. C.; Marron, D. F.; Weiler, R.; Guenther, E.; Parisi, J. Implantierbares System zur Anregung von Neuronen. German Patent DE102007020305A1, October 23, 2008.
(15) Monti, M. *J. Phys. Chem. C* **2007**, *111*, 6086−6099.
(16) Howse, J. R.; Steitz, R.; Pannek, M. P.; Simon, D. W.; Schubert, G. H.; Findenegg. *Phys. Chem. Chem. Phys.* **2001**, *3*, 4044−4051.
(17) Mezei, F.; Goloub, R.; Klose, F.; Toews, H. *Phys. B (Amsterdam)* **1995**, *213-214*, 898−900.
(18) Paul, A.; Krist, T.; Teichert, A.; Steitz, R. *Phys. B* **2011**, *406*, 1598−1606.
(19) Howse, J. R.; Manzanares-Papayanopoulos, E.; et al. *J. Chem. Phys.* **2002**, *116*, 172−178.
(20) Chazalviel, J. N.; Erne, B. H.; Maroun, F.; Ozanam, F. *J. Electroanal. Chem.* **2001**, *509*, 108−118.
(21) Kern, W. J. *Electrochem. Soc.* **1990**, *137*, 1887−1892.
(22) Roddick-Lanzilotta, A. D.; McQuillan, A. J. *J. Colloid Interface Sci.* **2000**, *227*, 48−54.
(23) Steitz, R.; Leiner, V.; Siebrecht, R.; von Klitzing, R. *Colloids Surf., A* **2000**, *163*, 63−70.

(24) Delajon, C.; Gutberlet, T.; Steitz, R.; Mohwald, H.; Krastev, R. *Langmuir* **2005**, *21*, 8509−8514.
(25) Soltwedel, O.; Ivanova, O.; Nestler, P.; Muller, M.; Kohler, R.; Helm, C. A. *Macromolecules* **2010**, *43*, 7288−7293.
(26) We had made the following assumptions in the initial stages of the fitting process for $Si/SiO_2/PEI/(dPSS/PAH)_8$: The scattering length density (SLD) of Si and SiO_2 were fixed at 2.07×10^{-6} Å^{-2} and 3.34×10^{-6} Å^{-2}. The SLD of the HDO (composed of 1:1 volume ratio of H_2O and D_2O) solvent was fixed at 2.9×10^{-6} Å^{-2} which is $(0.5 \times -0.56 \times 10^{-6} + 0.5 \times 6.37 \times 10^{-6})$ Å^{-2}. The SLD of PEM of PAH/dPSS soaked in pure D_2O solvent is known in literature to be about 5.5×10^{-6} Å^{-2}.[24] As our PEM were soaked in a HDO solvent, we initially fixed their SLD to 4×10^{-6} Å^{-2}. The average thickness (d) of a PAH/dPSS layer is known from other works to be about 47 Å when prepared from solutions with 2 M NaCl.[9] As our PEMs were prepared from solutions with 1 M NaCl, we expected a lower thickness and therefore, we initially fixed the thickness of the $Si/SiO_2/PEI/(dPSS/PAH)_8$ to 350 Å. SLD GA was fixed at 3.7×10^{-6} Å^{-2}. Roughness at all interfaces was set to 0 Å. Thickness of SiO_2 was first fitted and subsequently fixed at prior to the GA adsorption experiments. During the course of the subsequent fitting, we allowed parameters SLD of PEM, d of PEM, SLD of PE and d of PE to be optimized by the fitting procedure. Finally, we selected those values of the floated parameters of the PEM which corresponded to the best fit.
(27) Malmsten, M., Ed. *Biopolymers at Interfaces*: CRC Press: Boca Raton, FL, 2003.
(28) Horbett, T. A., Brash, J. L.,Eds. *Proteins at Interfaces II*; American Chemical Society: Washington, DC, 1995.
(29) Andrade, J. D., Ed. *Surface and Interfacial Aspects of Biomedical Polymers, Vol. 2 Protein Adsorption*; Plenum Press: New York, 1985.
(30) Roth, C. M.; Lenhoff, A. M. *Langmuir* **1995**, *11*, 3500−3509.
(31) Roth, C. M.; Lenhoff, A. M. *Langmuir* **1993**, *9*, 962−972.
(32) Norde, W. *Macromol. Symp.* **1996**, *103*, 5−18.
(33) Zhdanov, V. P.; Kasemo, B. *Langmuir* **2001**, *17*, 3518−3521.
(34) Ladam, G.; Gergely, C.; Senger, B.; Decher, G.; Voegel, J. C.; Schaaf, P.; Cuisinier, F. J. G. *Biomacromolecules* **2000**, *1*, 674−688.
(35) Robinson, S.; Williams, P. A. *Langmuir* **2002**, *18*, 8743−8748.
(36) Czeslik, C.; Jackler, G.; Steitz, R.; von Grunberg, H. *J. Phys. Chem. B* **2004**, *108*, 13395−13402.
(37) Sukhorukov, G. B.; Donath, E.; Lichtenfeld, H.; Knippel, E.; Knippel, M.; Budde, A.; Moehwald, H. *Colloids Surf. A* **1998**, *137*, 253−266.
(38) Schwinte, P.; Voegel, J. C.; Picart, C.; Haikel, Y.; Szalontai, B.; Schaaf, P. *J. Phys. Chem. B* **2001**, *105*, 11906−11916.
(39) Voets, I. K.; de Vos, W. M.; Hofs, B.; de Keizer, A.; Conhen Stuart, M. A.; Steitz, R.; Lott, D. *Phys. Chem. B* **2008**, *112*, 6937−6945.